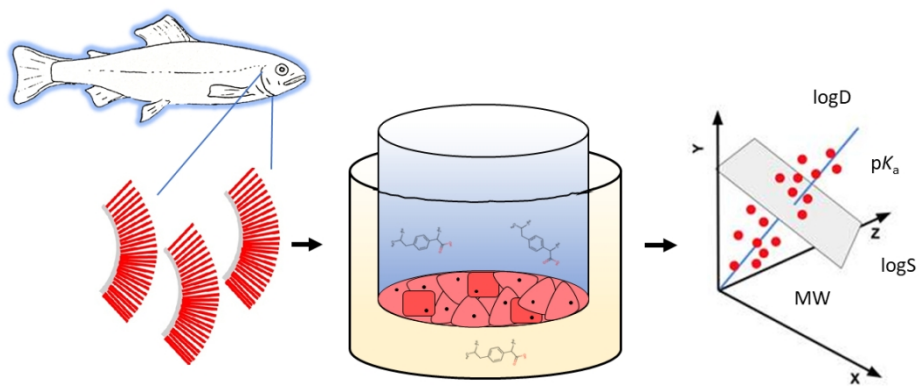


This document is the Accepted Manuscript version of a Published Work that appeared in final form in Environmental Science & Technology, copyright © 2018 American Chemical Society, after peer review and technical editing by the publisher. To access the final edited and published work see

<https://pubs.acs.org/doi/10.1021/acs.est.8b04394>



Graphic abstract

338x190mm (96 x 96 DPI)

18 **Abstract**

19

20 Modelling approaches, such as Quantitative Structure-Activity Relationships (QSARs) use
21 molecular descriptors to predict the bioavailable properties of a compound in biota. However,
22 these models have mainly been derived based on empirical data for lipophilic neutral
23 compounds and may not predict the uptake of ionizable compounds. The majority of
24 pharmaceuticals are ionizable and freshwaters can have a range of pH values that will affect
25 speciation. In this study we assessed the uptake of 10 pharmaceuticals (acetazolamide,
26 beclomethasone, carbamazepine, diclofenac, gemfibrozil, ibuprofen, ketoprofen,
27 norethindrone, propranolol and warfarin) with differing modes-of action and physicochemical
28 properties (pKa, logS, logD, logKow, molecular weight (MW) and polar surface area (PSA))
29 by an *in vitro* primary fish gill cell culture system (FIGCS) for 24 h in artificial freshwater.
30 Principal component analysis (PCA) and partial least squares (PLS) regression was used to
31 determine the molecular descriptors that influence the uptake rates. Ionizable drugs were
32 taken up by FIGCS and a strong positive correlation was observed between logS and a
33 negative correlation observed between pKa, logD, MW and the uptake rate. This approach
34 shows that models can be derived based on physicochemical properties of pharmaceuticals
35 and using an *in vitro* gill system to predict uptake of other compounds. There is a need for a
36 robust and validated model for gill uptake that could be used in a tiered risk assessment to
37 prioritize compounds for experimental testing.

38

39

40 Introduction

41

42 Pharmaceuticals are biologically active molecules that have been detected in surface waters
43 at ng to $\mu\text{g L}^{-1}$ concentrations¹ and are widely reported in aquatic fauna². The impacts
44 associated with pharmaceutical exposure on aquatic organisms is unclear and knowledge is
45 necessary to inform regulatory authorities and the pharmaceutical industry of compounds that
46 may pose a risk³.

47

48 As part of a chemical risk assessment it is necessary to determine the likelihood to
49 bioaccumulate. A bioconcentration factor (BCF) is a measure which includes uptake (k_1) and
50 elimination rates (k_2) and internal steady state concentration^{4,5}. However, the uptake process,
51 along with metabolism, represent the largest factors of uncertainty in fish bioaccumulation
52 models^{6,7}, and BCF values for individual compounds derived from *in vivo* studies can vary
53 substantially⁸. Consequently, a novel approach to evaluating the bioavailability properties of a
54 chemical has been proposed which utilizes non-guideline methodologies in a tiered risk
55 assessment⁸. In this approach, *in silico* or *in vitro* data may be used in the lower tiers to assess
56 a chemical's bioavailability; if there is enough information to classify bioaccumulation potential
57 then a decision can be made as to whether further BCF studies are required⁸.

58

59 Many mechanistic assessments of contaminant uptake are based on *in silico* models such as
60 Quantitative Structure-Activity Relationships (QSARs), that have largely been derived from
61 data for lipophilic neutral compounds that passively diffuse across lipid membranes and
62 undergo little to no metabolism⁶. QSAR can include linear based estimations or more recently
63 machine learning applications such as neural networks and tree-based learning to predict
64 organic chemicals bioconcentration⁹. However, an estimated 77.5% of pharmaceuticals are
65 ionizable¹⁰. Thus, the applicability of QSAR models developed on other contaminant classes
66 (i.e. neutral hydrophobic contaminants) may be limited and inaccurately estimate the
67 accumulation of pharmaceuticals. For compounds that are ionizable the acid-base

68 dissociation constant (pK_a) describes the dissociation of the drug at a given pH and influences
69 solubility, lipophilicity, permeability and protein binding¹¹. In the aquatic environment, surface
70 water pH will determine chemical speciation, and this is predicted to have an influence on
71 bioavailability¹². The typical pH of environmental water ranges between 6-9¹² although fish can
72 be found in bodies of water that are extremely acidic (pH 3)¹³ and highly alkaline (pH 10.5)¹⁴.
73 The effect of pH on the toxicity¹² and uptake/elimination of ionizable compounds in fish has
74 been demonstrated¹⁵⁻¹⁷. Recently, Bittner et al.¹⁸ have demonstrated the impact of pH (5.5 –
75 8.6) on the uptake and toxicity of beta-blocker pharmaceuticals in zebrafish larvae; where the
76 skin is likely to be the significant route of uptake. Karlsson et al.¹⁹ have examined the effect of
77 water and sediment pH (5.5 – 8.5 pH) on uptake of 3 pharmaceuticals uptake with a range of
78 pK_a (4.01 – 9.62 pK_a) in the freshwater oligochaete *Lumbriculus variegatus*.

79

80 There is a desire towards the development of *in vitro* models to replace or supplement current
81 animal experimental procedures²⁰, in accordance with the replacement, reduction, and
82 refinement (3Rs) principle²¹. This is also reflected in European legislature that states non-
83 animal alternative approaches should be used in place of animal procedures wherever
84 possible. A fish gill cell culture system (FIGCS) was developed using primary fish cells that
85 has shown promise as an alternative system for whole fish chemical uptake studies²². FIGCS
86 maintains many of the characteristics of the *in vivo* epithelium, including the presence of
87 multiple cell types associated with transport of ions across the gills and the ability to tolerate
88 freshwater water application to the apical surface. The *in vitro* data obtained from FIGCS
89 experiments has the potential to be an important component of the lower tier in a tiered testing
90 system⁸ as the gills are a primary route of uptake in fish²². It has recently been used to
91 investigate the absorption of 7 pharmaceuticals with a similar pK_a of 8.1 to 9.6 across the gill²³.

92

93 There is a paucity in fish pharmaceutical uptake and BCF values because the tests to derive
94 these use a large number of organisms, are time consuming and expensive to conduct. In this
95 study we assessed the uptake of 10 pharmaceuticals by an *in vitro* fish gill model with differing

106 physiochemical properties and there were three aims. Firstly, to assess the uptake of ionizable
107 pharmaceuticals by this fish gill epithelium. Secondly, to demonstrate how an *in vitro* epithelial
108 model can be used to evaluate the propensity for a drug to enter a fish from the water and
109 how this information could form part of a tiered risk assessment approach^{8,24}. Thirdly, Lipsinki
110 et al.²⁵ proposed that the molecular properties (molecular weight, hydrogen bond donors and
111 acceptors and $\log K_{ow}$) of a chemical can be used as a screening tool to determine the
112 likelihood of absorption across a membrane, we extended this concept and used the
113 pharmaceutical molecular descriptors and partial least squares (PLS) regression analysis to
114 model uptake rate and identify those descriptors that influence gill uptake. We were able to
115 show that solubility, pKa, octanol-water distribution coefficient and molecular weight are the
116 most important descriptors driving epithelial drug uptake rates.

107

108 **Materials and Methods**

109

110 **Fish gill cell culture system (FIGCS)**

111

112 Juvenile rainbow trout (*Oncorhynchus mykiss*) were obtained from a local trout farm and
113 housed in dechlorinated-aerated City of London tap water ($[Na^+]=0.53\text{mM}$, $[Ca^{2+}]=0.92\text{mM}$,
114 $[Mg^{2+}]=0.14\text{mM}$, $[K^+] = 0.066 \text{ mM}$ and $[NH_4^+] = 0.027 \text{ mM}$). Temperature was maintained at
115 14°C with a 14h light:10h dark cycle and fish were fed a 1% (w/v) ration of trout pellets daily.

116

117

118 Primary fish gill cell culture inserts were prepared in companion wells and maintained
119 according to protocols described in Schnell et al.²². The transepithelial resistance (TER) was
120 monitored daily using an epithelial tissue voltohmmeter (EVOMX) with STX-2 chopsticks
121 (World Precision Instruments). A TER value of above $3,000\Omega \text{ cm}^{-2}$ was used as criteria for the

122 presence of a tight epithelium, as previously determined using ^{14}C -mannitol as a paracellular
123 permeability marker²³.

124

125 **Pharmaceuticals exposures and cell viability assay**

126

127 Analytical grade pharmaceuticals (purity $\geq 97\%$) from differing classes of action with differing
128 chemical properties (Table 1) were purchased from Sigma Aldrich, and included
129 acetazolamide (CAS: 59-66-5), beclomethasone (CAS: 4419-39-0), carbamazepine (CAS:
130 298-46-4), diclofenac sodium salt (CAS: 15307-79-6), gemfibrozil (CAS: 25812-30-0),
131 ibuprofen sodium salt (CAS: 31121-93-4), ketoprofen (CAS: 22071-15-4), norethindrone-19
132 (CAS: 68-22-4), propranolol hydrochloride (CAS: 318-98-9) and warfarin (CAS: 81-81-2).
133 Pharmaceutical stocks were prepared at a concentration of 1 mg mL^{-1} in methanol or ethanol
134 and stored at -80°C .

135

136 Following formation of a tight epithelium inserts were prepared for exposure by washing with
137 phosphate buffered saline. The apical freshwater (AFW) used for apical exposure was
138 prepared according to OECD₂₀₃ Test Guidelines²⁶ (2 mM CaCl_2 ; 0.5 mM MgSO_4 ; 0.8 mM
139 NaHCO_3 , 77.1 μM KCl, with a measured pH 7.6) with individual pharmaceuticals added at a
140 concentration of $1 \mu\text{g mL}^{-1}$, which is equivalent to: 450 nM acetazolamide, 245 nM
141 beclomethasone, 423 nM carbamazepine, 338 nM diclofenac, 399nM gemfibrozil, 485 nM
142 ibuprofen, 393 nM ketoprofen, 355 nM norethindrone, 386 nM propranolol, and 324 nM
143 warfarin. To expose cells 1.5 mL of exposure water was added to the apical compartment and
144 2 mL of L15 media with 5% FBS to the basal compartment. The inserts, and 1.5 mL exposure
145 water samples (T_0) were incubated at 18°C in the dark for 24 hrs. In the case of the T_0 samples
146 this was to assess if the compounds remained stable over the 24 hrs exposure period at 18°C
147 in the absence of cells. The T_0 and the 1.5 mL apical compartment water samples after 24 hrs
148 exposure (T_{24}) were collected and stored at -80°C for further analysis. Measurements were

149 made on 4 inserts derived from 2 to 3 biological replicates, with each biological replicate
150 comprising of cells harvested from 2 fish.

151

152 To consider the adhesion of the compounds to the companion well and insert membrane
153 during 24 hrs of exposure, a cell-free experiment was performed. To assess pharmaceutical
154 toxicity, single seeded primary gill cells were grown in T75 flasks to 80% confluent, then
155 trypsinized and transferred to 96-well at a density of 1×10^5 cells well⁻¹. Twenty-four hours post-
156 seeding in the 96-well plates cells were exposed to pharmaceuticals at $1 \mu\text{g mL}^{-1}$ in L15 with
157 5% FBS for 24 hours, after which a MTT viability assay 3-(4,5-dimethylthiazol-2-yl)-2,5-
158 diphenyltetrazolium bromide) was performed following methods adapted from Riss et al.²⁷. pH
159 stability of the AFW with $1 \mu\text{g mL}^{-1}$ of compound was measured with and without cells and found
160 to be stable over a 24 hour period.

161 **HPLC Analysis**

162

163 For HPLC analysis individual T_0 or T_{24} samples were pooled into three separate mixtures: Mix
164 A included beclomethasone, ibuprofen and warfarin, Mix B included carbamazepine,
165 diclofenac, gemfibrozil, ketoprofen and norethindrone and Mix C included acetazolamide and
166 propranolol for solid phase extraction (SPE) with Oasis HLB cartridges (200mg sorbent, 6cc).
167 Cartridges were initially conditioned with 6 mL methanol (HPLC grade) followed by 6 mL water
168 (HPLC grade) then loaded with either pooled sample Mix A, B or C. Cartridges were washed
169 with 4 mL water, dried under vacuum pressure and eluted with 6 mL methanol or stored at -
170 80°C for later elution. Samples were then dried under nitrogen at 45°C for 80 min (Biotage
171 TurboVap), reconstituted in 500 μL 90:10 (v/v) water:acetonitrile and vortexed for 2 minute
172 before transfer to amber HPLC vial for analysis.

173

174

175 Liquid chromatography was performed on an Agilent 1260 Infinity series LC system using a
176 Waters Sunfire C₁₈ column (100 Å, 3.5 μm , 4.6 mm x 150 mm) at a flow rate of 0.2 mL min^{-1}

177 and injection volume of 20 μL . Mobile phase A and B consisted of HPLC grade water and
178 HPLC grade acetonitrile, respectively, with initial running conditions of 10% phase B at a
179 column temperature of 40 $^{\circ}\text{C}$. The gradient elution was as follows; linear ramp with phase B
180 increased to 80% at 12 min, held for 13 min, then returned to initial conditions at 28 min. Total
181 run time was 40 min including a 12 min re-equilibration period. An Agilent 1290 Infinity Diode
182 Array Detector was used for detection of diclofenac and warfarin at 214 nm; carbamazepine,
183 ibuprofen and gemfibrozil at 220 nm; beclomethasone and propranolol at 230 nm;
184 norethindrone at 254 nm; ketoprofen at 263 nm and acetazolamide at 273 nm.

185
186 Method performance was assessed by matrix-matched calibration curves generated for the
187 AFW. Method linearity (5 concentrations, $n=3$) was determined from 0.5 -2.5 $\mu\text{g mL}^{-1}$ and
188 signal to noise ratio of 3:1 and 10:1 of low concentration spiked samples was used to
189 determine the LOD and LOQ, respectively ($n=6$). Precision was determined using spiked
190 samples at 1 $\mu\text{g mL}^{-1}$ ($n=6$) and accuracy was determined using spiked samples and values
191 from method linearity ($n=6$). Recovery was assessed by comparing spiked samples (pre-
192 extraction) to post-extract spiked samples at a concentration of 0.5, 1 or 2 $\mu\text{g mL}^{-1}$ ($n=3$).

193

194 **Estimation of Gill Uptake Rates**

195

196 Primary gill cell culture pharmaceutical uptake was calculated based on the loss of compound
197 from the apical compartment corrected for the amount that adhered to the polystyrene plastic
198 of the companion wells and inserts without cells over 24 hrs (Equation 1).

199

$$200 \text{ Uptake rate (nmol cm}^{-2} \text{ h}^{-1}) = (T_0 - T_{24}) - (T_0^p - T_{24}^p) / (t \times \text{cm}^2) \quad \text{Eqn. 1}$$

201

202 Where T_0 and T_{24} represents the moles (nmoles) of drug present in the apical compartment in
203 the presence of cells at 0 and 24 hrs, respectively, and T_0^p and T_{24}^p represent the moles of
204 drug present in the apical compartment in the absence of cells at 0 h and 24 h, respectively;

205 t = time of the flux measurement (24 hrs) and cm^2 represents the surface area of the epithelium
206 (0.9 cm^2). Sorption controls (inserts and exposure media only) were setup to account for any
207 losses of compound through volatilization, sorption to plastics and any other degradative
208 processes. Insert controls showed that these processes were negligible and therefore in the
209 presence of cells disappearance of compound is related to the uptake of the compound into
210 the gill epithelium and transfer across into the basolateral layer over 24 hours.

211

212 **Statistics and Modelling Approaches**

213

214 A one-way ANOVA followed by a Tukey's post hoc test was performed to compare the uptake
215 rates of each compound using GraphPad Prism 6.0. Modelling approaches used 6 molecular
216 descriptors (Table 1) including; the acid dissociation constant ($\text{p}K_{\text{a}}$), the octanol water
217 distribution coefficient at pH 7.4 ($\log D$), the octanol-water partition coefficient ($\log K_{\text{ow}}$), polar
218 surface area (PSA) and molecular mass (M_{w}). The two descriptors $\log K_{\text{ow}}$ and $\log D$ are both
219 measures of hydrophobicity, but $\log D$ takes into account both neutral and ionizable species at
220 a given pH whereas $\log K_{\text{ow}}$ only takes into account the neutral fraction. Principle component
221 analysis (PCA) and partial least squares (PLS) regression were performed using the R
222 statistical computing language, R version 3.4.3 (freely available at <https://www.r-project.org/>).
223 All scripts were written with RStudio (freely available at <https://www.rstudio.com/>), packages
224 used for PCA and PLS analysis were *stats* and *plsdepot*, respectively. Full dataset used in
225 modelling, latent variable scores, loadings, weights and cross-validation of models are given
226 in the SI (Figure S3 and Tables S4-S7). For cross-validation of the PLS model, a leave-one-
227 out approach was used.

228

229 **Results**

230

231 Cell viability was assessed by MTT assay and none of the pharmaceuticals at a concentration
232 of $1 \mu\text{g mL}^{-1}$ showed signs of cytotoxicity (Supporting Information (SI), Figure S1) and HPLC
233 method performance assessment is provided in the supplementary data (SI Table S1 and S2).

234

235 Pharmaceutical adhesion to the companion wells over 24 hrs was between 0.7 to 5% (data
236 not shown) and was taken into consideration when calculating uptake rates. Acetazolamide
237 uptake ($0.125 \pm 0.032 \text{ nmoles cm}^{-2} \text{ h}^{-1}$) was significantly greater than beclomethasone,
238 carbamazepine, diclofenac and norethindrone (beclomethasone $0.021 \pm 0.015 \text{ nmoles cm}^{-2} \text{ h}^{-1}$,
239 carbamazepine $0.022 \pm 0.004 \text{ nmoles cm}^{-2} \text{ h}^{-1}$, norethindrone $0.024 \pm 0.003 \text{ nmoles cm}^{-2}$
240 h^{-1} , diclofenac $0.027 \pm 0.003 \text{ nmoles cm}^{-2} \text{ h}^{-1}$) (Figure 1). The other ionizable drugs, except for
241 diclofenac, showed higher, but not significantly higher uptake rates (ibuprofen 0.072 ± 0.013
242 $\text{ nmoles cm}^{-2} \text{ h}^{-1}$, gemfibrozil $0.075 \pm 0.007 \text{ nmoles cm}^{-2} \text{ h}^{-1}$, ketoprofen $0.061 \pm 0.006 \text{ nmoles}$
243 $\text{ cm}^{-2} \text{ h}^{-1}$, propranolol, $0.095 \pm 0.026 \text{ nmoles cm}^{-2} \text{ h}^{-1}$ and warfarin $0.070 \pm 0.012 \text{ nmoles cm}^{-2}$
244 h^{-1}) compared to the neutral drugs, beclomethasone, carbamazepine, and norethindrone
245 (Figure 1, and SI Figure S2).

246

247 Modelling of the molecular descriptors was performed using PCA analysis to identify
248 compound similarity (Fig 2). The first two principal components explained a cumulative
249 variance of 69% (PC1 = 48%, PC2 = 21%) in the descriptor space. The score plot indicates
250 that there were no apparent outliers in the dataset. Clustering of compounds was minimal but
251 was expected with the low number of cases available for modelling (n=10). The largest
252 variation in the descriptor space was observed for the compound beclomethasone (Fig. 2).
253 The variance of this case can be explained in terms of the loadings, where this compound was
254 the largest (MW = 408.92) and most hydrophobic ($\log D = 4.16$) of all compounds that were
255 tested. From the descriptor loadings, $\log S$ and MW were negatively correlated with each other.
256 The loadings for the first latent variable also showed that $\log D$ (0.567), MW (0.505), $\log S$ (-
257 0.444) and pK_a (0.407) were more important variables than $\log K_{ow}$ (0.201) or PSA (0.146).

258

259 PLS was implemented to interpret molecular descriptors that influence gill uptake rates of
260 pharmaceuticals and enable a predictive modelling approach with:

261

$$\text{Uptake Rate (nmoles cm}^{-2} \text{ h}^{-1}) = 1.23\text{E-}01 + (-1.59\text{E-}03 \times \text{p}K_{\text{a}}) + (1.53\text{E-}02 \times \log\text{S}) + (-7.26\text{E-}03 \times \log\text{D}) + (9.15\text{E-}03 \times \log K_{\text{ow}}) + (-9.48\text{E-}05 \times \text{MW}) + (3.83\text{E-}04 \times \text{PSA}) \quad \text{Eqn.}$$

264 2

265

266 The adjusted correlation coefficient (R^2_{adj}) and the cross-validated R^2 (Q^2) of the PLS
267 regression model was 0.7863 and 0.5397, respectively. No cases were observed as outliers
268 in the PLS model determined by the Hotelling's T^2 95% confidence ellipse (data not shown).
269 Based on the cumulative Q^2 statistic (see SI Figure S4), the optimal number of latent variables
270 for the PLS model was two. The loadings plot (Figure 3a) indicated that logS was positively
271 correlated with gill uptake whereas logD, $\text{p}K_{\text{a}}$ and MW were negatively correlated with gill
272 uptake. The $\log K_{\text{ow}}$ and PSA descriptors were relatively less important for modelling gill uptake
273 when compared with the previously mentioned descriptors. The use of PLS to predict gill
274 uptake showed good performance with the mean absolute error of $0.01 \pm 0.01 \text{ nmol cm}^{-2} \text{ h}^{-1}$
275 (MAE \pm SD) for all compounds tested. Larger inaccuracies in the predictions were observed for
276 the four compounds; carbamazepine (122%), diclofenac (61%), norethindrone (35%) and
277 propranolol (32%) (Fig 3b and c).

278

279 Discussion

280

281 The uptake rate of 10 pharmaceuticals by a fish primary gill cell culture system was
282 assessed. From our dataset we were able to demonstrate that a PLS regression model based
283 on the drug molecular descriptors could be developed for pharmaceutical uptake rate by this
284 epithelium, with LogS, $\text{p}K_{\text{a}}$, logD and MW found to be the most important descriptors driving
285 epithelial drug uptake rates.

286

287 The uptake rates of the compounds from the apical compartment reflect the apparent epithelial
 288 permeability (P_{app}) of the compound by the FIGCS cells. The P_{app} can be expressed as an
 289 equation (equation 3) and takes into consideration four factors: partitioning in the aqueous
 290 boundary layer (P_{ABL} , ABL), adhesion to filter insert (P_f) and transcellular (trans) or paracellular
 291 (para) transfer (P_{trans} , P_{para})²⁸. The aqueous boundary layer is assumed to have a distinct
 292 boundary with the bulk water adjacent to both sides of the membrane²⁹.

293

295

$$\frac{1}{P_{app}} = \frac{1}{P_{ABL}} + \frac{1}{P_f} + \frac{1}{P_{trans} + P_{para}} \quad \text{Eqn. 3}$$

296

297 Two of the four factors can be discounted, due to the nature of the system. Firstly, adhesion
 298 to plastic (P_f) and inserts was taken into consideration when calculating the uptake rate.
 299 Secondly, a previous study conducted using the paracellular marker ¹⁴C-mannitol determined
 300 that at TER values above 3,000Ω cm² the FIGCS were relatively impermeable to the marker
 301 and indicated that transport was via transcellular routes²³, all compounds in the current study
 302 have a greater molecular weight than mannitol thus paracellular transfer (P_{para}) was negligible.
 303 Thus, the uptake rates reflect partitioning in the ABL (P_{ABL}), uptake into cells and across the
 304 basolateral membrane (P_{trans}) into the basolateral compartment, in addition to any potentially
 305 metabolized compound efflux from the gill cells back into apical compartment.

306

307 All uptake studies were conducted in AFW and under these conditions acetazolamide (71.5%),
 308 diclofenac (100.0%), gemfibrozil (99.9%), ibuprofen (99.8%), ketoprofen (99.9%), propranolol
 309 (98.5%) and warfarin (99.7%) are all predicted to be ionized (% ionized in parentheses),
 310 whereas beclomethasone, carbamazepine, and norethindrone are not ionized. All ionizable
 311 drugs, except diclofenac, showed higher permeation into the primary gill cell epithelium when
 312 compared to the neutral drugs (Figure 1). The observation that ionizable drugs are capable of
 313 permeating the gill epithelium corroborates a previous study in FIGCS concerning the uptake
 314 of a set of pharmaceuticals with pK_a between 8.1- 9.6²³ and a number of studies suggest that
 315 ionizable compounds can be taken up by the fish gill^{e.g. 15,16,18,19,23,30,31}. The uptake of 9 weakly

316 acidic chlorinated phenols by rainbow trout did not vary between pH 6.3 to 8.4 despite the
317 proportion of the compounds ranging in ionization from 1 to 99 %¹⁵, the accumulation of the
318 weak basic diphenhydramine (pK_a 9.1) at $10 \mu\text{g L}^{-1}$ reached steady state in fathead minnow
319 at pH 7.73 and 8.63 after ~24 h and only at pH 6.87 was accumulation greatly reduced³¹ and
320 ionizable surfactant³², perflouroakyl acids³³ as well as phenols and carboxylic acids³⁴ have
321 been observed to cross the gills of fish. However, membrane permeation may be an order of
322 magnitude less than for the neutral form³⁰. Erickson et al.,¹⁶ developed a mechanistic model
323 of ionized organic chemical uptake at the fish gill which expanded on an original model for
324 unionized chemical uptake^{35,36}. This new model included a factor that takes into account the
325 ability of the fish to alter the pH adjacent to the apical membrane and thus generating a
326 microclimate that differs to the bulk water³⁷. These changes in pH at the gill surface helped to
327 explain uptake of diphenylamine³¹ and the chlorinated phenols^{15,16}. However, in the current
328 study uptake of the acidic and basic pharmaceuticals showed similar uptake rates, and if
329 uptake is solely due to the neutral form of the drug, then pH of the culture epithelial
330 microclimate would have to be in the region of pH 3 to ensure the weakly acidic drugs (pK_a 4
331 – 5.08) were unionized. It is also unlikely that uptake is solely due to the ionized form because
332 the basic drugs show similar uptake rates (Figure 1 and ²³). In contrast to the other ionizable
333 compounds, diclofenac is the only drug that exhibited a relatively lower uptake rate. It is
334 unclear why this may be, but of the drugs used in the current study the structure of diclofenac
335 is more complex containing both an amine and carboxylic acid group and lacks conformational
336 flexibility³⁸ that may influence transport by the gill epithelium.

337

338 The PLS modelling approach showed that all descriptors here have an influence on the uptake
339 rate but more of the explained variance was correlated to the logS, logD, pK_a and MW
340 descriptors. The regression model (Equation 2) showed a good potential to predict uptake
341 rates in the FIGCS system at the tested concentration and water chemistry ($r^2 = 0.786$).
342 Modelling is an important aspect to understanding fate of pharmaceuticals in the aquatic
343 environment and these approaches are complementary to *in vitro* systems for the replacement

344 of animal testing. Comparison to *in vivo* fish uptake rates would be useful, however there are
345 a limited number of studies reporting these values. We have collated those 'steady state'
346 plasma concentrations for 9 of the 10 pharmaceuticals in the supplemental file (SI Table S8),
347 but note that the complexity and variation in pH, exposure, species, size and temperature
348 make direct comparison to our data difficult. Furthermore, these studies do not allow us to
349 derive uptake rates and therefore are not suitable for comparison with our dataset. Predicted
350 K_1 , LC_{50} and BCF values can be derived from QSAR models for fish (SI, Table S8). However,
351 a poor correlation was observed between the predicted K_1 , LC_{50} and BCF and our *in vitro*
352 pharmaceutical uptake rates (Table S8), emphasizing the need for alternative models for these
353 compounds. To fully validate the model a much larger number of compounds would be
354 needed. A robust and validated model for gill uptake could then be used as a pre-screen to
355 prioritize compounds for experimental testing in a tiered approach⁸. In this scenario if a
356 compound is predicted to not be bioavailable in *in vitro* studies and other information from
357 lower tier screens support this observation, then further BCF testing in living fish may not be
358 required^{8,24}.

359

360 The pharmaceutical uptake rate was most strongly positively correlated to logS (Figure 2b)
361 suggesting that this physiochemical property facilitates access of the pharmaceuticals to the
362 cells and uptake. The ABL in multi-well plates is between 1,000 – 2,000 μm and forms a
363 significant diffusional barrier³⁹ where by the concentration in bulk solution exceeds that located
364 at the membrane surface. Increased solubility aids permeability across the ABL²⁹ allowing for
365 greater interaction with the membrane⁴⁰. Carbamazepine was expected to have a higher
366 uptake based on solubility, as well as being neutral and hydrophobic, but influx rates were low
367 and carbamazepine had the largest prediction inaccuracy in the PLS regression model. The
368 reason for this is uncertain. Carbamazepine has a low BCF value in adult zebrafish (BCF_{ss} of
369 $1.41 \pm 7.13 \text{ L kg}^{-1}$) but this is likely associated with greater biotransformation capacity and
370 clearance rather than a significant reduction in uptake when compared to other pharmaceutical
371 and personal care products tested¹⁷. Whether the gills actively excrete carbamazepine back

372 into the apical water compartment remains to be determined. Carbamazepine's mode of action
373 is promiscuous, and it interacts with different types of receptors and channels⁴¹. However, the
374 main target is voltage gated Na⁺ channels located on the surface of the cells⁴¹ where it acts
375 as a competitive inhibitor by allosteric inhibition⁴². A possibility is that in our system the drug
376 adheres to and interacts with the surface and related channels but does not permeate into the
377 cell.

378

379 A negative correlation of uptake rates with logD was observed. The gill membrane consists of
380 a range of phospholipids (e.g. phosphatidylethanolamines and phosphatidylcholine) with
381 differing properties capable of forming electrostatic and hydrogen bonds with charged
382 molecules. It has been shown that ionized drugs can partition into artificial lipid membranes
383 greater than predictions based on logK_{ow}⁴⁴ and there is a positive relationship between the
384 dipole potential in the region between the aqueous phase and the interior membrane bilayer
385 allowing permeation of ionized compounds in these synthetic membranes^{24,45,46}. This
386 phenomenon gave rise to the pH-piston hypothesis to explain sorption of ionized drugs into
387 artificial vesicles consisting of dioleoylphosphatidylcholine, due to electrostatic interactions with
388 acidic and basic drugs⁴⁵ and may explain how the ionized compounds are able to cross the
389 membrane.

390

391 The PLS regression also indicated that the uptake rates were negatively correlated with MW.
392 MW is known to play a distinct role in cellular uptake of solutes and has been used successfully
393 to model permeability of both neutral and charged molecules, in addition to be a component
394 of Lipinski's rule of 5 in drug discovery^{43,47,48}. The LogK_{ow} and PSA accounted for some of the
395 variance in the regression but to a much less extent than the other molecular descriptors.

396

397 The role of transport proteins in ionizable drug uptake is axiomatic^{e.g. 49-51}, but the extent of the
398 role transport proteins play in drug uptake is debated. Kell and colleagues proposed that
399 uptake is almost solely due to transport proteins⁵², though this has been strongly questioned⁵³.

400 In our current study all flux rates were measured at concentrations that far exceed
401 environmental concentrations and it is likely that carrier mediated transport processes were
402 saturated. Here we are measuring both the passive and facilitated uptake, with passive
403 dominating and entry likely via electrostatic interactions with the phospholipid membrane of
404 the fish gill²⁴. But, several organic, anion, cation or zwitterion transporters are present at the
405 gill e.g. *slco1d1*⁵⁵, OATP⁵⁶ and *slc15a2*⁵⁷, and their ability to facilitate drug uptake from the
406 water requires further understanding. An alternative explanation for the uptake of charged
407 molecules is transportation as ion pairs⁵⁸, a property that has been utilized to assist in
408 developing drug penetration for a number of epithelia, such as the ocular epithelium⁵⁹ and the
409 skin⁶⁰, but has not been considered for fish gill epithelial. Natural water contains numerous
410 potential counterions and the fish excretes ions and other charged molecules from the gill that
411 could form ion-pairs with charged drugs.

412

413 **Environmental Implications**

414 The current study shows that the FIGCS can be used to assess drug uptake by fish gills from
415 the water in accordance with previous studies²³. It also shows that ionizable drugs are able to
416 cross the gill epithelium, but further work is required to ascertain the significance of the gill
417 microclimate at the apical membrane, ion pairing, electrostatic interactions (between the
418 ionized pharmaceutical and the membrane phospholipids) and transport proteins on ionizable
419 compound transport. A PLS regression model based on the physicochemical properties of the
420 drug was used to predict uptake rate (the model accounted for 78% of the explained variance)
421 where logS, pK_a, logD and MW were significant drivers. To fully validate the model a much
422 larger number of compounds would be needed, however, this approach shows that modelling
423 can be used to understand the uptake of pharmaceuticals by an *in vitro* epithelium system that
424 could replace whole animals in bioaccumulation studies. There is a need a robust and
425 validated model for gill uptake could then be used as a pre-screen to prioritize compounds for
426 experimental testing in a tiered risk assessment⁸ where compounds that do not cross the gill
427 epithelia may not need further costly and time-consuming animal testing.

428

429 **Acknowledgements**

430 This work was conducted under funding awarded to NRB from the Biotechnology and
431 Biological Sciences Research Council (BBSRC) CASE industrial scholarship scheme
432 (Reference BB/M014827/1), and AstraZeneca Global SHE research programme.
433 AstraZeneca is a biopharmaceutical company specializing in the discovery, development,
434 manufacturing and marketing of prescription medicines, including some products reported
435 here. SFO is an employee of AstraZeneca and his time represents an AstraZeneca
436 contribution in kind to the Innovative Medicines Initiative Joint Undertaking under grant
437 agreement no. 115735 – iPiE: Intelligent led assessment of Pharmaceuticals in the
438 Environment, resources of which are composed of financial contribution from the European
439 Union's Seventh Framework Programme (FP7/2015-2018) and European Federation of
440 Pharmaceutical Industries and Associations (EFPIA) companies' in kind contribution.

441

442 **Supporting Information.**

- 443 • Cytotoxicity of the pharmaceuticals in primary gill cells (MTT assay)
- 444 • *in vivo* BCF data from literature
- 445 • QSAR predictions of K_1 , LC_{50} and BCF
- 446 • HPLC method performance assessment
- 447 • Linear regression analysis of uptake rates in relation to the chemical descriptors
448 modelling supplementary information including scores, loadings, modified weights and
449 cross-validation for PCA and PLS.

450

451 **References**

- 452 (1) Halm-Lemeille, M.P.; Gomez, E. Pharmaceuticals in the environment. *Environ. Sci. Pollut.*
453 *Res.* **2016**, *23*, 4961-4963.
- 454 (2) Miller, T.H.; Bury, N.R.; Owen, S.F.; MacRae, J.I.; Barron, L.P. A review of the
455 pharmaceutical exposome in aquatic fauna. *Environ. Pollut.* **2018**, *239*, 129 – 146.

- 456 (3) Lockwood, S.; Saïdi, N. Background document for public consultation on pharmaceuticals
457 in the environment. Interim report for European Commission contract number:
458 07.0201/2015/721866/SER/ENV.C.1.2017; [https://ec.europa.eu/info/sites/info/files/backgroun](https://ec.europa.eu/info/sites/info/files/background_document_public_consultation_pharmaceuticals_environment.pdf)
459 [d_document_public_consultation_pharmaceuticals_environment.pdf](https://ec.europa.eu/info/sites/info/files/background_document_public_consultation_pharmaceuticals_environment.pdf).
- 460 (4) Arnot, J.A.; Gobas, F.A.P.C. A Review of Bioconcentration Factor (BCF) and
461 Bioaccumulation Factor (BAF) Assessments for organic chemicals in aquatic organism.
462 *Environ. Rev.* **2006**, *14*, 257-297.
- 463 (5) OECD test number 305, Bioaccumulation in Fish: Aqueous and Dietary Exposure.
464 <https://doi.org/10.1787/9789264185296-en>.
- 465 (6) Nichols, J.; Erhardt, S.; Dyer, S.; James, M.; Moore, M.; Plotzke, K.; Segner, H.; Schultz,
466 I.; Thomas, K.; Vasiluk, L.; Weisbrod, A. Use of *In Vitro* Absorption, Distribution, Metabolism,
467 and Excretion (ADME) data in bioaccumulation assessments for fish. *Hum. Ecol. Risk*.
468 *Assess.* **2007**, *13*, 1164-1191.
- 469 (7) Nichols, J.; Fay, K.; Bernhard, M.J.; Bischof, I.; Davis, J.; Halder, M.; Hu, J.; Johanning,
470 K.; Laue, H.; Nabb, D.; Schleichriem, C.; Segner, H.; Swintek, J.; Weeks, J.; Embry, M.
471 Reliability of In Vitro Methods Used to Measure Intrinsic Clearance of Hydrophobic Organic
472 Chemicals by Rainbow Trout: Results of an International Ring Trial. *Toxicol. Sci.* **2018**, *164*,
473 563-575.
- 474 (8) Lillicrap, A.; Springer, T.; Tyler, C.R. A tiered assessment strategy for more effective
475 evaluation of bioaccumulation of chemicals in fish. *Regul. Toxicol. Pharm.* **2016**, *75*, 20-26.
- 476 (9) Miller, T.H.; Gallidabino, M.D.; MacRae, J.I.; Owen, S.F.; Bury, N.R.; Barron, L.P.
477 Prediction of bioconcentration factors in fish and invertebrates using machine learning. *Sci.*
478 *Total Environ.* **2019**, *648*, 80-89.
- 479 (10) Manallack, D.T. The pKa distribution of drugs: Application to drug discovery. *Perspec.*
480 *Medicin. Chem.* **2007**, *1*, 25-38.
- 481 (11) Manallack, D.T.; Prankerd R.J.; Yuriev E.; Oprea T.I.; Chalmers D.K. The significance of
482 acid/base properties in drug discovery. *Chem. Soc. Rev.* **2013**, *42*, 485-496.
- 483 (12) Boström, M.L.; Berglund, O. Influence of pH-dependent aquatic toxicity of ionizable
484 pharmaceuticals on risk assessments over environmental pH ranges. *Water Res.* **2015**, *72*,
485 154-161.
- 486 (13) Duarte, R.M.; Smith, S.D.; Val, A.L.; Wood, C.M. Dissolved organic carbon from the upper
487 Rio Negro protects zebrafish (*Danio rerio*) against ionoregulatory disturbances caused by low
488 pH exposure. *Sci. Rep.* **2016**, *6*, 20377.
- 489 (14) Ford, A.G.P.; Dasmahapatra, R.K.; Rüber, L.; Gharbi, K.; Cezard, T.; Day J.J. High levels
490 of interspecific gene flow in an endemic cichlid fish adaptive radiation from an extreme lake
491 environment. *Mol. Ecol.* **2015**, *24*, 3421-3440.
- 492 (15) Erickson, R.J.; McKim, J.M.; Lien, G.J.; Hoffman, A.D.; Batterman, S.L. Uptake and
493 elimination of ionizable organic chemicals at fish gills: I. Model formulation, parameterization,
494 and behavior. *Environ. Toxicol. Chem.* **2006**, *25*, 1512-1521.

- 495 (16) Ericksson, R.J.; McKim, J.M.; Lien, G.J.; Hoffman, A.D.; Betterman, S.L. Uptake and
496 elimination of ionisable organic chemicals at fish gills: II. Observed and predicted effects of
497 pH, alkalinity, and chemical properties. *Environ. Toxicol. Chem.* **2006**, *25*, 1522-1532.
- 498 (17) Chen, F.; Gong, Z.; Kelly, B.C. Bioaccumulation behavior of pharmaceuticals and
499 personal care products in adult zebrafish (*Danio rerio*): Influence of physical-chemical
500 properties and biotransformation. *Environ. Sci. Technol.* **2017**, *51*, 11085-11095.
- 501 (18) Bittner, L.; Teixido, E.; Seiwert, B.; Escher, B.I.; Klüver, N. Influence of pH on the uptake
502 and toxicity of β -blockers in embryos of zebrafish, *Danio rerio*. *Aquat Toxicol.* **2018**, *201*, 129-
503 137.
- 504 (19) Karlsson, M.V.; Carter, L.J.; Agatz, A.; Boxall, A.B.A. Novel approach for characterizing
505 pH-dependent uptake of ionizable chemicals in aquatic organisms. *Environ. Sci. Technol.*
506 **2017**, *51*, 6965 – 6971.
- 507 (20) Wolf, W.D.; Comber, M.; Douben, P.; Gimeno, S.; Holt M.; Leonard, M.; Lillicrap, A.; Sijm,
508 D.; Egmond, R.V.; Weisbrod, A.; Whale, G. Animal use Replacement, Reduction, and
509 Refinement: Development of an integrated testing strategy for bioconcentration of chemicals
510 in fish. *Integr. Environ. Assess. Manag.* **2007**, *3*, 3-17.
- 511 (21) Lillicrap, A.; Belanger, S.; Burden, N.; Du Pasquier, D.; Embry, M.R.; Hlader, M.; Lampi,
512 M.A.; Lee, L.; Norberg-King, T.; Rattner, B.A.; Schirmer, K.; Thomas, P. Alternative
513 approaches to vertebrate ecotoxicity tests in the 21st Century: A review of developments over
514 the last 2 decades and current status. *Environ. Toxicol. Chem.* **2016**, *35*, 2637-2646.
- 515 (22) Schnell, S.; Stott, L.C.; Hogstrand, C.; Wood, C.M.; Kelly, S.P.; Pärt, P.; Owen, S.F.; Bury,
516 N.R. Procedures for the reconstruction, primary culture and experimental use of rainbow trout
517 gill epithelia. *Nat. Protoc.* **2016**, *11*, 490-498.
- 518 (23) Stott, L.C.; Schnell, S.; Hogstrand, C.; Owen, S.F.; Bury, N.R. A primary fish gill cell
519 culture model to assess pharmaceutical uptake and efflux: Evidence for passive and facilitated
520 transport. *Aquat. Toxicol.* **2015**, *159*, 127-137.
- 521 (24) Armitage, J.M. ; Erickson, R.J. ; Luckenbach, T. ; Ng, C.A.; Prosser, R.S. ; Arnot, J.A. ;
522 Schirmer, K.; Nichols, J.W. Assessing the bioaccumulation potential of ionizable organic
523 compounds: current knowledge and research priorities. *Environ. Toxicol. Chem.* **2017**, *36*,
524 882-897.
- 525 (25) Lipinski, C.A.; Lombardo, F.; Dominy, B.W.; Feeney, P.J. Experimental and
526 computational approaches to estimate solubility and permeability in drug discovery and
527 development settings. *Adv. Drug Deliver. Rev.* **1997**, *23*, 3 - 25.
- 528 (26) OECD test number 203, Fish, acute toxicity test. [https://doi.org/10.1787/9789264069961-](https://doi.org/10.1787/9789264069961-en)
529 [en](https://doi.org/10.1787/9789264069961-en).
- 530 (27) Riss, T.L.; Moravec, R.A.; Niles, A.L.; Duellman, S.; Benink, H.A.; Worzella, T.J.; Minor,
531 L. 2013. Assay Guidance Manual: Cell Viability Assays.
532 <https://www.ncbi.nlm.nih.gov/books/NBK144065/>.
- 533 (28) Avdeef, A. *Absorption and drug development: solubility, permeability, and charge state*;
534 John Wiley & Sons: Hoboken, NJ., 2012.

- 535 (29) Karlsson, J.; Artursson, P. A method for the determination of cellular permeability
536 coefficients and aqueous boundary layer thickness in monolayers of intestinal epithelial (Caco-
537 2) cells grown in permeable filter chambers. *Int. J. Pharm.* **1991**, *71*, 55-64.
- 538 (30) Armitage, J.M.; Arnot, J.A.; Wania, F.; Mackay, D. Development and evaluation of a
539 mechanistic bioconcentration model for ionogenic organic chemicals in fish. *Environ. Toxicol.*
540 *Chem.* **2013**, *32*, 115-128.
- 541 (31) Nichols, J.W.; Du, B.; Berninger, J.P.; Connors, K.A.; Chambliss, C.K.; Erickson, R.J.;
542 Hoffman, A.D.; Brooks, B.W. Observed and modelled effects of pH on bioconcentration of
543 diphenhydramine, a weakly basic pharmaceutical, in fathead minnow. *Environ. Toxicol. Chem.*
544 **2015**, *34*, 1425-1435.
- 545 (32) Tolls, J.; Kloepper, A.M.S.; Sijm, D.T.H.M. Surfactant bioconcentration – A critical review.
546 *Chemosphere* **1994**, *29*, 693 – 717.
- 547 (33) Furdui, V.I.; Stock, N.L.; Ellis, D.A.; Butt, C.M.; Whittle, D.M.; Crozier, P.W.; Reiner,
548 E.J.; Muir, D.C.G.; Mabury, S.A. Spatial distribution of perfluoroalkyl contaminants in lake trout
549 from the Great Lakes. *Environ. Sci. Technol.* **2007**, *41*, 1554-1559.
- 550 (34) Saarikoski, J.; Lindstrom, M.; Tynnila, M.; Viluksela, M. Factors affecting the absorption
551 of phenolics and carboxylic acids in the guppy (*Poecilia reticulata*). *Ecotoxicol. Environ. Saf.*
552 **1986**, *11*, 158-173.
- 553 (35) Erickson, R.J.; McKim, J.M. A model for exchange of organic chemicals at fish gills: flow
554 and diffusion limitations. *Aquat. Toxicol.* **1990**, *18*, 175-198.
- 555 (36) McKim, J.M.; Erickson, R.J. Environmental impacts on the physiological mechanisms
556 controlling xenobiotic transfer across fish gills. *Physiol. Zool.* **1991**, *64*, 39-67.
- 557 (37) Wood, C.M. 2001. Toxic Responses of the Gill. In: Schlenk D. and Benson W.H. (Eds),
558 Target Organ Toxicity In Marine and Freshwater Teleosts, vol. I. Taylor and Francis, London,
559 pp.1-89.
- 560 (38) Harrold, M.W.; Zavod, R.M. Chapter 2: Functional Group Characteristics and Roles. In
561 *Basic Concepts in Medicinal Chemistry*; Harrold, M. W., Zavod, R. M.; American Society of
562 Health-System Pharmacists: Maryland 2013; pp. 15-50.
- 563 (39) Shibayama, T.; Morales, M.; Zhang, X.; Martinez, L.; Berteloot, A.; Secomb, T.W.; Wright,
564 S.H. Unstirred Water Layers and the Kinetics of Organic Cation Transport. *Pharm. Res.* **2015**,
565 *32*, 2937-2949.
- 566 (40) Savjani, K.T.; Gajjar A.K.; Savjani J.K. Drug Solubility: Importance and Enhancement
567 Techniques. *ISRN Pharmacol.* **2012**, 2012, 1-10.
- 568 (41) Ambrosio, A.F.; Soares da Silva, P.; Carvalho, C.M.; Carvalho, A.P. Mechanisms of
569 Action of Carbamazepine and Its Derivatives: Oxocarbazepine, BIA 2-093, and BIA 2-024.
570 *Neurochem. Res.* **2002**, *27*, 121-130.
- 571 (42) Willow, M.; Kuenzel, E.A.; Catterall, A. inhibition of voltage-sensitive sodium channels in
572 neuroblastoma cells and synaptosomes by the anticonvulsant drugs diphenylhydantoin and
573 carbamazepine. *Mol. Pharmacol.* **1983**, *25*, 228-234.

- 574 (43) Bhal, S.K.; Kassam, K.; Peirson, I.G.; Pearl, G.M. The rule of five revisited: Applying LogD
575 in place of LogP in drug-likeness filters. *Mol. Pharmaceutics*. **2007**, *4*, 556-560.
- 576 (44) Foradada, M.; Esterlrich, J. Encapsulation of thioguanine in liposomes. *Int. J.*
577 *Pharmaceutics*. **1995**, *124*, 261-269.
- 578 (45) Avdeef, A.; Box, K.J.; Comer, J.E.A.; Hibbert, C.; Tam, K.Y. pH-metric LogP 10.
579 Determination of liposomal membrane-water partition coefficients of ionisable drugs. *Pharm.*
580 *Res*. **1998**, *15*, 209 – 215.
- 581 (46) Escher, B.I.; Schwarzenbach, R.P.; Westall, J.C. Evaluation of liposome-water
582 partitioning of organic acids and bases. 1. Development of sorption model. *Environ. Sci.*
583 *Technol*. **2000**, *34*, 3954-3961.
- 584 (47) Camenisch, G.; Alsenz, J.; van de Waterbeemd, H.; Folkers, G. Estimation of permeability
585 by passive diffusion through Caco-2 cell monolayers using the drugs lipophilicity and
586 molecular weight. *Eur. J. Pharm. Sci*. **1998**, *6*, 313-319.
- 587 (48) Pagliara, A.; Reist M.; Geinoz S.; Carrupt P.A.; Testa B. Evaluation and prediction of drug
588 permeation. *J. Pharm. Pharmacol*. **1999**, *51*, 1339-1357.
- 589 (49) Dobson, P. D.; Kell, D. B. Carrier-mediated cellular uptake of pharmaceutical drugs: an
590 exception or the rule? *Nat. Rev. Drug Discov*. **2008**, *7*, 205–220.
- 591 (50) Giacomini, K.M.; Huang, S.M.; Tweedie, D.J.; Benet, L.Z.; Brouwer, K.L.; Chu, X.; Dahlin,
592 A.; Evers, R.; Fischer, V.; Hillgren, K.M.; Hoffmaster, K.A.; Ishikawa, T.; Keppler, D.; Kim,
593 R.B.; Lee, C.A.; Niemi, M.; Polli, J.W.; Sugiyama, Y.; Swaan, P.W.; Ware, J.A.; Wright,
594 S.H.; Yee, S.W.; Zamek-Gliszczynski, M.J.; Zhang, L. Membrane transporters in drug
595 development. *Nat. Rev. Drug. Discov*. **2010**, *9*, 215-236.
- 596 (51) Nigam, S. What do drug transporters really do? *Nat.Rev.Drug. Discov*. **2015**, *14*, 29-44.
- 597 (52) Kell, D.B.; Oliver, S.G. How drugs get into cells: tested and testable predictions to help
598 discriminate between transporter-mediated uptake and lipoidal bilayer diffusion. *Front.*
599 *Pharmacol*. **2014**, *5*, 231.
- 600 (53) Smith, D.; Artursson, P.; Avdeef, A.; Di, L.; Ecker, G.F.; Faller, B.; Houston, J.B.; Kansy,
601 M.; Kerns, E.H.; Kramer, S.D.; Lennemas, H.; van de Waterbeemd, H.; Sugano, K.; Testa, B.
602 Passive lipoidal diffusion and carrier-mediated cell uptake are both important mechanisms of
603 membrane permeation in drug disposition. *Mol. Pharm*. **2014**, *11*, 1727-1738.
- 604 (54) Zolk, O.; Solbach, T.F.; Konig, J.; Fromm, M.F. Functional characterization of the human
605 organic cation transporter 2 variant p.270ala > ser. *Drug Metab. Dispos*. **2009**, *37*, 1312-1318.
- 606 (55) Popovic, M.; Zaja, R.; Fent, K.; Smital, T. Interaction of environmental contaminants with
607 zebrafish organic anion transporting polypeptide, Oatp1d1 (Slco1d1). *Toxicol. Appl.*
608 *Pharmacol*. **2014**, *280*, 149-158.
- 609 (56) Popovic, M.; Zaja, R.; Smital, T. Organic anion transporting polypeptides (OATP) in
610 zebrafish (*Danio rerio*): Phylogenetic analysis and tissue distribution. *Comp. Biochem.*
611 *Physiol*. **2010**, *155A*, 327-335.

- 612 (57) Romano, A.; Kottra, G.; Barca, A.; Tiso, N.; Maffia, M.; Argenton, F.; Daniel, H.; Storelli,
 613 C.; Verri, T. High-affinity peptide transporter PEPT2 (SLC15A2) of the zebrafish *Danio rerio*:
 614 functional properties, genomic organization, and expression analysis. *Physiol. Genomics*
 615 **2006**, *24*, 207-217.
- 616 (58) Neubert, R. Ion pair transport across membranes. *Pharm. Res.* **1989**, *6*, 743-747.
- 617 (59) Sasaki, H; Yamamura, K; Mukai, T; Nishida, K.; Nakamura, J.; Nakashima, M.; Ichikawa,
 618 M. Enhancement of ocular drug penetration. *Crit. Rev. Ther. Drug* **1991**, *16*, 85-146.
- 619 (60) Hui, M. ; Quan, P. ; Yang, Y.Y. ; Fang, L. 2016. The effect of ion-pair formation combined
 620 with penetration enhancers on the skin permeation of loxoprofen. *Drug Deliv.* **2016**, *23*, 1550-
 621 1557.

622

623

624

625

626

627

628

629

630

631

632 **Table 1:** Pharmaceutical molecular descriptors.

633

	pK _a	logS	Molecular Weight (g mol ⁻¹)	logD	logK _{ow}	PSA (Å ²)	% ionisation at pH 7.6
Acetazolamide	7.20	-2.36	222.24	0.23	3.48	115.04	71.5
Beclomethasone	13.85	-5.4	408.92	4.16	3.49	106.97	0
Carbamazepine	15.96	-3.2	236.27	2.28	2.28	46.33	0
Diclofenac	4.00	-4.8	296.15	1.22	1.9	52.16	100
Gemfibrozil	4.42	-4	250.33	1.40	4.77	46.53	99.9
Ibuprofen	4.91	-3.5	206.28	0.29	2.48	40.10	99.8
Ketoprofen	4.45	-4.1	254.28	0.06	0.97	54.37	99.9
Norethindrone	17.59	-4.7	298.40	2.98	3.15	37.30	0
Propranolol	9.42	-3.5	259.34	1.29	3.09	41.49	98.5
Warfarin	5.08	-3.8	308.32	0.16	0.85	63.60	99.7

634

635

636

637

638 **Figure 1:** Pharmaceutical uptake rate into the fish gill cell culture system. Values represent
639 average of 4 inserts derived from between 4 -6 fish. Bars with differing letters are significantly
640 different from each other when compared via a One-way ANOVA followed by a Tukey's post-
641 hoc test, $p < 0.05$.

642
643
644

645 **Figure 2:** PCA biplot showing the first two principal component (PC1 and PC2) loadings and
646 scores for each molecular descriptor and case, respectively. Scores are indicated on the first
647 axes (left and bottom, black) loadings are indicated by the second axes (right and top, red). A
648 -acetazolamide; B – beclomethasone; C- carbamazepine; D – diclofenac; G – gemfibrozil; I –
649 ibuprofen; K - ketoprofen; N – norethindrone; P – propranolol and W – warfarin.

650

651 **Figure 3:** PLS regression analysis showing (A) loadings of the first two latent variables for
652 molecular descriptors (independent variables) and uptake rate (dependent variable) (B)
653 predicted versus observed gill uptake rates using PLS regression model (C) raw residuals of
654 predicted uptake rates.

655

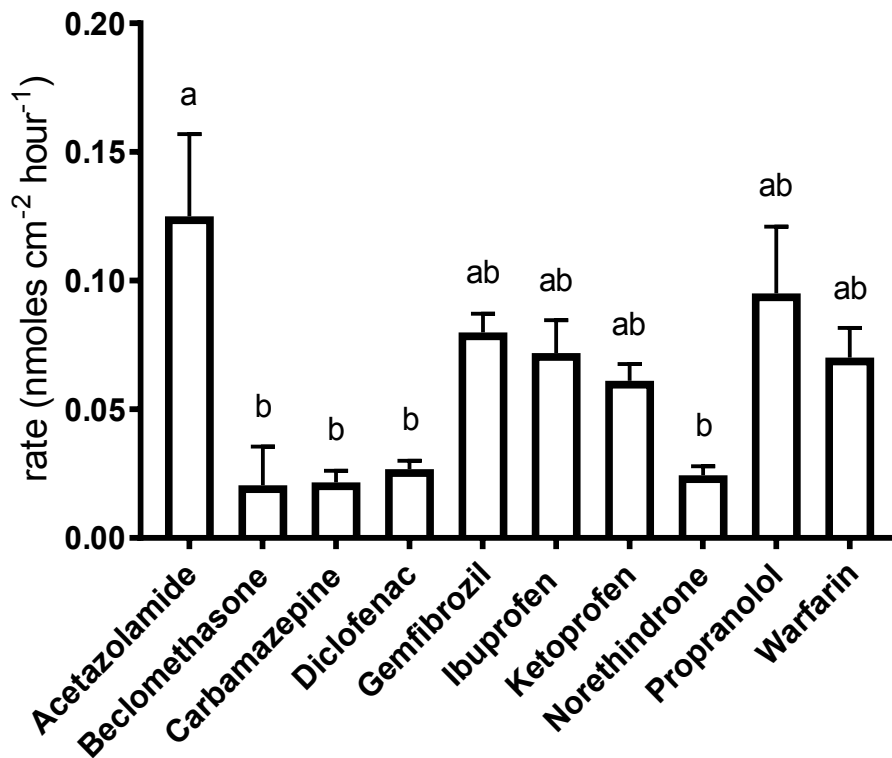
656 **Figure 1**

657

658

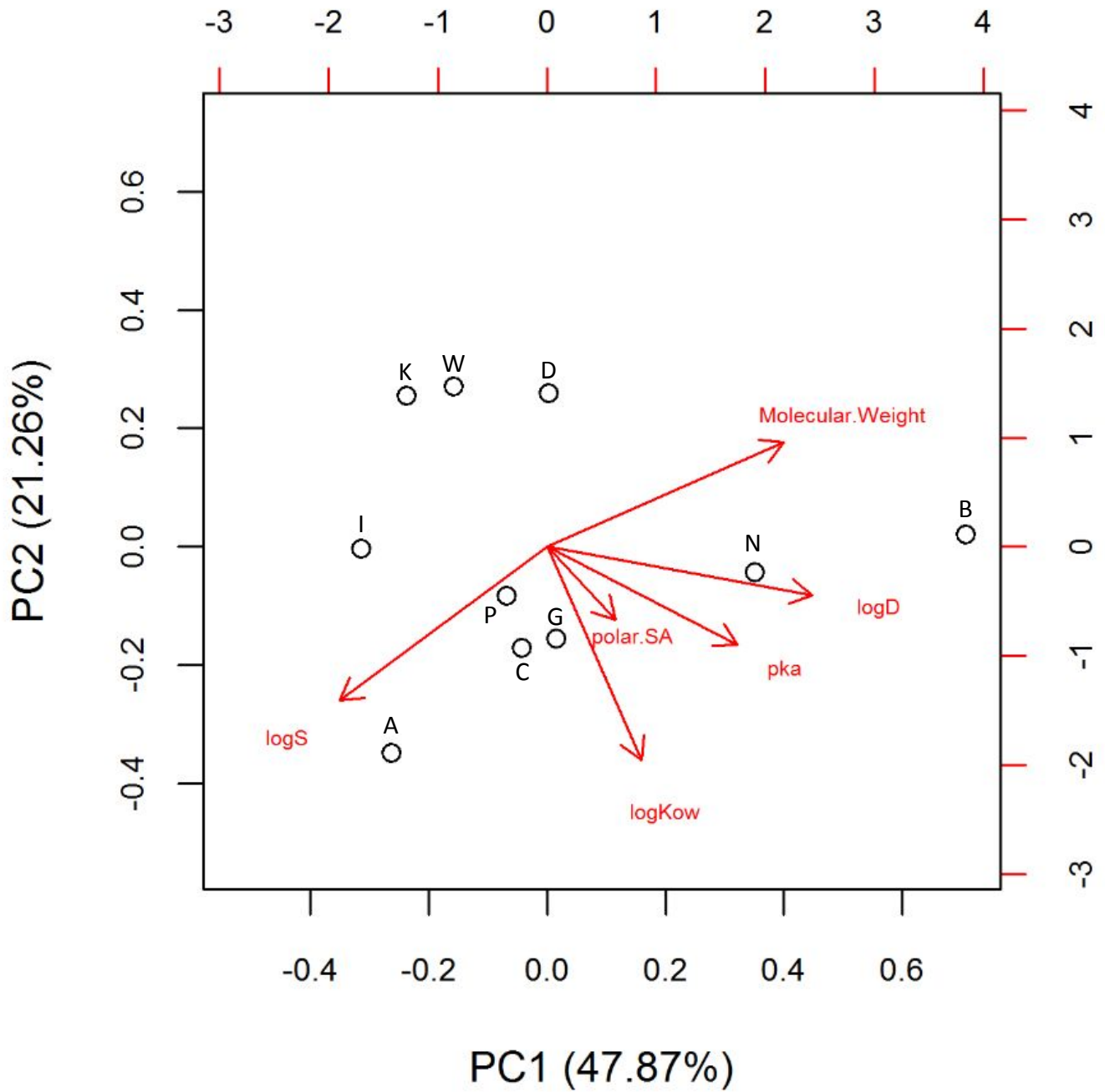
659

660



661

662

663 **Figure 2**

664

665 **Figure 3**

666

667

